Protein Science (1997), 6:1375–1386. Cambridge University Press. Printed in the USA.
Copyright © 1997 The Protein Society

Conformational substates in enzyme mechanism: The 120 K structure of α-lytic protease at 1.5 Å resolution

STEPHEN D. RADER[1] AND DAVID A. AGARD[2]

[1]Graduate Group in Biophysics
[2]Howard Hughes Medical Institute and Department of Biochemistry and Biophysics, University of California at San Francisco, San Francisco, California 94143-0448

(RECEIVED November 25, 1996; ACCEPTED March 19, 1997)

Abstract

Insight into the dynamic properties of α-lytic protease (αLP) has been obtained through the use of low-temperature X-ray crystallography and multiple-conformation refinement. Previous studies of αLP have shown that the residues around the active site are able to move significantly to accommodate substrates of different sizes. Here we show a link between the ability to accommodate ligands and the dynamics of the binding pocket. Although the structure of αLP at 120 K has *B*-factors with a uniformly low value of 4.8 Å^2 for the main chain, four regions stand out as having significantly higher *B*-factors. Because thermal motion should be suppressed at cryogenic temperatures, the high *B*-factors are interpreted as the result of trapped conformational substates. The active site residues that are perturbed during accommodation of different substrates are precisely those showing conformational substates, implying that substrate binding selects a subset of conformations from the ensemble of accessible states. To better characterize the precise nature of these substates, a protein model consisting of 16 structures has been refined and evaluated. The model reveals a number of features that could not be well-described by conventional *B*-factors: for example, 40% of the main-chain residue conformations are distributed asymmetrically or in discrete clusters. Furthermore, these data demonstrate an unexpected correlation between motions on either side of the binding pocket that we suggest is a consequence of "dynamic close packing." These results provide strong evidence for the role of protein dynamics in substrate binding and are consistent with the results of dynamic studies of ligand binding in myoglobin and ribonuclease A.

Keywords: α-lytic protease; *B*-factor; cryocrystallography; dynamics; plasticity; serine protease; substrate specificity; thermal expansion

α-Lytic protease (αLP, E.C. 3.4.21.12) is an extracellular bacterial serine protease from *Lysobacter enzymogenes* (Whitaker et al., 1966). Its crystal structure revealed that, despite a low level of sequence similarity (18% identity to elastase), it adopts the same three-dimensional fold as the chymotrypsin family of pancreatic serine proteases (Brayer et al., 1979). αLP preferentially cleaves substrates on the C-terminal side of small hydrophobic residues, such as Ala and Val. This specificity is determined primarily by the three residues whose side chains form the S1 pocket (active site nomenclature according to Schechter & Berger, 1967)—Met 190, Met 213, and Val 218.[3] Mutation of these residues has dramatic effects on the specificity of αLP (Bone et al., 1989a, 1989b, 1991a). In particular, the mutant Met 190 → Ala (MA190) is able to cleave substrates with residues ranging in size from Ala to Phe at the P1 position with increased activity relative to the wild-type enzyme with its best substrate (Bone et al., 1989b). Other parts of the protein also play an important role in defining the substrate specificity profile for the enzyme, including distant residues (up to 21 Å from the active site serine) in the "omega loop," which includes residues 216–226 (Mace et al., 1995). Crystallographic analysis of wild-type α-lytic protease and binding pocket mutants complexed with numerous peptide boronic acid inhibitors suggests that the conformational adaptability of residues around the active site is critical to determining the specificity of the enzyme (Bone et al., 1987, 1989a, 1989b, 1991a, 1991b; Mace & Agard 1995; Mace et al., 1995).

The use of peptide boronic acid inhibitors has been crucial for our structure–function analyses. These peptidic inhibitors, which terminate with a boronic acid instead of a carboxylic acid, are good mimics of the tetrahedral transition state or nearby tetrahedral intermediates in protein hydrolysis (Kettner et al., 1988). They

Reprint requests to: David A. Agard, Department of Biochemistry and Biophysics, University of California at San Francisco, San Francisco, California 94143-0448; e-mail: agard@msg.ucsf.edu.

[3]Residues in α-lytic protease are numbered by homology to chymotrypsin according to the alignment of Fujinaga et al. (1985). Insertions in the sequence are indicated by suffix letters, e.g., the first residue is Ala 15A, the second Asn 15B. Consequently, mutations are denoted with both amino acids (in single-letter code) before the residue number, for example the Met 190 → Ala mutation is denoted MA190.

show extremely tight binding to native and mutant proteins (e.g., K_I = 0.35 nM for Boc-Ala-Pro-boroVal to wild-type αLP, where boroVal is the boronic acid analogue of valine; Kettner et al., 1988), and there is an excellent correlation between the $\log(1/K_I)$ of the inhibitors and the $\log(k_{cat}/K_m)$ for the corresponding substrates (Bone et al., 1991a; Mace & Agard, 1995), indicating that interactions between the enzyme and these inhibitors are similar to those between the enzyme and the transition state for substrate hydrolysis.

Crystal structures of complexes between boronic acid inhibitors and α-lytic protease revealed fundamental features of the catalytic transition state. They confirmed the tetrahedral geometry of the atom bound to the active site serine and demonstrated that the catalytic histidine is ideally positioned to donate a proton to the leaving group (Bone et al., 1987). Additionally, complexes of the boronic acid inhibitors with binding-pocket mutations revealed that the protein is capable of significant conformational changes in both main-chain and side-chain atoms in order to accommodate substrates of varying sizes. These conformational changes are localized to regions around the binding pocket and represent ligand-induced perturbations. Surprisingly, this structural adaptability is not manifested as high crystallographic temperature factors (*B*-factors) in relevant regions of the free or inhibited enzymes. This suggests that the mobile residues are not simply flexible (moving in a broad energy minimum with no barriers), but instead are plastic (populating a number of closely spaced, discrete conformational energy wells; Bone et al., 1989b), as schematized in Figure 1. Flexibility then represents vibrational motion within an energy well, whereas plasticity allows for fluctuations between discrete energy wells.

It now seems clear that the specificity of α-lytic protease is determined by the way in which binding pocket atoms respond to the presence of ligands, in other words, by the energetic costs of the conformational changes required to accommodate different ligands. Furthermore, the crystallographic studies suggest that these perturbations manifest themselves as discrete energy minima near to the native state. The crucial question for understanding α-lytic protease function is whether these distorted configurations are part of the ensemble of low-energy configurations in the unliganded, native protease. We address this question with an analysis of the dynamics of α-lytic protease using a combination of cryocrystallography and multiple-conformation refinement. It is important to understand that, by protein dynamics, we refer specifically to small deviations from mean atomic positions, driven by thermal energy. Larger-scale motions—allosteric changes, motor protein conformational changes, etc.—are not being considered because they are widely recognized to play an important role in protein function. By contrast, the importance of local dynamics to enzyme function needs to be carefully investigated.

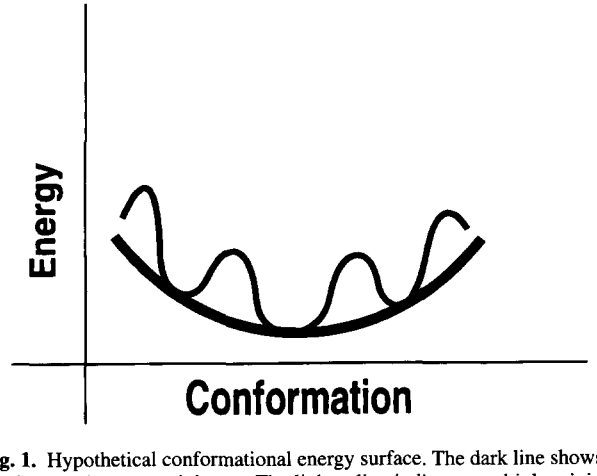

Fig. 1. Hypothetical conformational energy surface. The dark line shows a single, broad energy minimum. The lighter line indicates multiple minima over the same conformational space. Flexible atoms vibrate within a single minimum, whereas "plastic" atoms fluctuate among multiple minima.

Although X-ray crystal structures are generally thought of as static, the atomic *B*-factors provide a mechanism for extracting dynamic information. As the temperature of a protein crystal is changed, only the dynamic, or thermal, contribution to the atomic *B*-factors should be affected (Frauenfelder et al., 1979). The difference in *B*-factors (ΔB-factor) between two temperatures therefore gives a measure of the accessible displacements, or flexibility, of each atom. Hartmann et al. (1982) have shown that the atomic motion of some atoms in myoglobin extrapolates to the zero-point value [$\langle u_x^2 \rangle$ = 0.01 Å^2, determined from small molecule data (Willis & Pryor, 1975)] at T = 0 K, but, for other atoms, it extrapolates to a larger value, indicating the existence of conformational substates.

Frauenfelder et al. (1979) provided evidence from the temperature-dependence of the *B*-factors that there is little plasticity in myoglobin, although there are many accessible substates. Without these dynamic modes, oxygen would be unable to penetrate to or be released from the heme. Additionally, Rasmussen et al. (1992) showed that ribonuclease A loses its activity when the temperature drops below 200 K, a temperature at which collective motions in proteins have been shown to freeze out. These results demonstrate that protein dynamics are readily accessible to crystallographic observation and suggest that they are important for protein function.

Given the probable existence of conformational substates at cryogenic temperatures, some alternative to using a single model of the protein with isotropic *B*-factors is required. This problem already exists in the determination of high-resolution structures at room temperature where multiple, discrete side-chain conformations are often seen. Where no clear discrete configurations are visible, disorder is typically modeled implicitly via an increase in the atomic *B*-factors. By contrast, we have chosen to use multiple-conformation refinement, in which several models of the protein are refined simultaneously in an effort to explicitly model all aspects of conformational heterogeneity.

Multiple conformation refinement has been used previously on crambin, ribonuclease (Kuriyan et al., 1991), and mannose-binding protein A (Burling et al., 1996) to improve the protein model and to demonstrate conformational substates. In both of these studies, however, the atomic *B*-factors were also refined along with each of the models. To a first approximation, this is inconsistent with the underlying physics for structures at 120 K. Although the substates can, in principle, have further substates whose distribution could be approximated using individual *B*-factors, the differences in *B*-factors due to these second-order effects are likely to be much smaller than what can be modeled reliably. Other studies of the behavior of proteins at cryogenic temperatures (Hartmann et al., 1982; Earnest et al., 1991), as well as our data, indicate that thermal motion is reduced at these temperatures to a level corresponding to a *B*-factor of 2–4 Å^2. The observation of *B*-factors higher than this must indicate static disorder (Frauenfelder et al., 1979; Hartmann et al., 1982)—i.e., multiple conformations. In order to model configurational heterogeneity correctly, we have set all atomic *B*-factors for the protein to the value of the average *B*-factor for the protein main chain *in a multiple-conformation model* (3.5 Å^2),

which forces the shape of the electron density to be modeled by the distribution of the atomic coordinates for the multiple models.

The results presented here demonstrate the existence of conformational substates that correlate with the discrete conformations seen in previous structures and provide a physical basis for plasticity. We also observe correlated motion of residues around the binding pocket, which helps explain the specificities of binding pocket mutants.

Results

The 120 K structure

Statistics for the data collection and crystallographic refinement are shown in Table 1. No intensity cut-off was applied to the data during refinement. The unit cell dimensions of the frozen crystals are only 0.8% smaller than the room temperature values (2ALP, $a = b = 66.3$, $c = 80.1$; Fujinaga et al., 1985). There is a 0.61° rotation and 0.4 Å translation in the atomic coordinates between the 298 and 120 K structures. The final *R*-factor for the single 120 K structure is 16.5% with data from 6.0 to 1.5 Å (Table 2). The geometry is excellent, with RMS deviations (RMSDs) in bond lengths of 0.009 Å and angles of 1.9°. Ramachandran plots indicate that all non-glycine residues are in favored regions of phi-psi space with five exceptions (data not shown). The five exceptions (A39, N60, P95, T54, and P120) have been noted previously (Fujinaga et al., 1985) and are either in turns or just outside the boundary of favored locations in the Ramachandran plot. The RMSD of C_αs from 2ALP is 0.15 Å, indicating that the protein backbones are indistinguishable within experimental error.

The 0.8% decrease in cell dimensions for αLP on cooling from 298 K to 120 K corresponds to a 1.5% decrease in cell volume, smaller than the changes reported for any other protein studied to date (see Table 3). On cooling to 120 K, αLP shows very little thermal contraction, in contrast to the more helical proteins that have been studied previously (Frauenfelder et al., 1987; Earnest et al., 1991; Tilton et al., 1992; Young et al., 1994).

In order to quantitate the overall changes to the structure of α-lytic protease that occur on cooling, we have calculated the linear thermal expansion coefficient as described by Frauenfelder et al. (1987). To do this, the distance of each atom from the center of mass (C.O.M.) was calculated at both temperatures and then the difference between those distances *for each atom* was taken (Fig. 2). If there were no expansion of the protein, these differences would simply reflect coordinate error and the distribution would be centered precisely at 0. As Figure 2 shows, there is a small but systematic shift to larger distances as the temperature is increased. The distribution has a mean of +0.025 Å for 1,391 distances (all non-hydrogen protein atoms), compared to a shift of +0.16 Å for metmyoglobin. The average linear thermal expansion coefficient at 298 K, calculated from the observed expansion data using the solid-state approximation with a Debye temperature of 180 K, is 24×10^{-6} K^{-1} (for a fuller explanation, see Frauenfelder et al., 1987). This value is 4.8-fold lower than the corresponding value for myoglobin (Table 3), and indicates that αLP's thermal expansion coefficient is more similar to aluminum [$\alpha(300\text{ K}) = 24 \times 10^{-6}$ K^{-1}] than to other proteins for which it has been measured. Additionally, the radius of gyration of αLP decreases on cooling by only 0.13%, which is again a smaller change than observed previously (Table 3).

Table 1. *Data collection statistics for α-lytic protease*

Temperature (K)	120
Space group	$P3_221$
Unit cell (*a*, *c*) (Å)	65.8, 79.5
Unit cell volume (Å^3)	298,000
Total reflections	148,867
Unique reflections	31,458
Limiting resolution (Å)	1.50
Completeness (%)	99.0
R_{symm} (%)	5.9
Wilson *B*-factor (Å^2)	5.8
Mean atomic *B*-factor (Å^2)	5.36

The thermal changes can also be detected in the number of intermolecular contacts. At 298 K, αLP has 40 residues, or 92 atoms, that are involved in crystal contacts ($d < 4.0$ Å) with five other molecules (Fig. 3). When the temperature is decreased to 120 K, the number of residues at crystal contacts increases to 49 and the number of atoms increases to 144. The changes in crystal contacts and the 0.4-Å shift in the C.O.M. explain how the unit cell lengths can change by as much as 0.8% when the thermal expansion of the protein is so small. These changes in crystal contacts are similar to the changes observed in other proteins (Table 3), suggesting that crystal packing responds independently of the changes occurring within the protein.

The increased resolution and lower *B*-factors of the 120 K structure allow significantly more detail of the solvent structure to be ascertained than was possible at 298 K. The 298 K structure includes 156 water molecules and two sulfates (Fujinaga et al., 1985). We have modeled 300 water molecules, three sulfates, and one Tris molecule in the low-temperature structure. The Tris molecule is in the active site, near the active site serine (S195) and a sulfate. We have tried modeling the electron density as a peptide, but the very strong density for two of the hydroxyethyl groups clearly precludes this. Electron density is not visible for the hydroxyl groups of the Tris, however, the group occupancy refines to 0.79 with *B*-factors between 7 and 11 Å^2. The occupancy for 11 of the water molecules refined to values higher than 1.2 (with the highest refining to 2.32), but these were reset to 1.0 for the final analysis. Although this may suggest that some of these putative waters are actually sulfates (because there are no other high Z molecules in the crystals), the shape of the electron density is inconsistent with this interpretation. The average *B*-factor for the waters is 18.4 Å^2.

Ten side chains in the 120 K structure each have two discrete conformations in the electron density, which we have modeled explicitly. The residues so modeled are R90, S107, S110, S120G, S120H, R141, T161, R178, R192, and N219B. The group occupancy of the alternate conformations was adjusted over several cycles of refinement to minimize the *B*-factor difference between the two conformations. The resulting occupancies range from a 50:50 ratio to a 30:70 ratio, whereas the *B*-factors vary from 5 to 20 Å^2, depending on the residue. This is a considerable decrease from the *B*-factors calculated using a single side-chain conformation, which were generally 30% higher.

B-factors and multiple conformation analysis

The premise of this work is that the change in *B*-factors (Δ*B*-factors) with temperature is a good metric for protein flexibility at

Table 2. *Refinement statistics for the single- and multiple-structure models of α-lytic protease at 120 K*

Number of structures in model	1	16
Resolution range for refinement (Å)	6.0–1.5	6.0–1.5
R-factor (%)	16.5	15.5
Free *R*-factor (%)	19.2	18.9
Bond length deviation (Å)	0.009	0.007
Bond angle deviation (Å)	1.86	1.70
Residues in disallowed phi-psi regions (%)	2.5	2.5
Non-hydrogen protein atoms	1,477	22,256
$\langle B \rangle$ (Å^2) (all atoms)	5.36	3.47[a]
$\langle B \rangle$ (Å^2) (protein main chain)	4.79	3.47[a]
RMSD[b] non-hydrogen atoms (Å)	—	0.315
RMSD[b] backbone (Å)	—	0.205

[a]All *B* values set to the mean value for backbone atoms of the 16-structure model with refined *B*s.
[b]RMSDs calculated from mean atomic position.

room temperature. Mossbauer spectroscopy (Hartmann et al., 1982) and small molecule data (Willis & Pryor, 1975), as well as theoretical considerations, show that atoms at 120 K have an RMS displacement due to thermal motion of less than 0.2 Å (corresponding to a *B*-factor of 3.2 Å^2 according to the relation $B_i = 8\pi^2 \langle u_x^2 \rangle$, where $\langle u_x^2 \rangle$ is the mean square displacement of atom *i* in the direction *x*). Given the small *B*-factors at 120 K, the Δ*B*-factors between the 298 K and 120 K structures should represent the true thermal component of the *B*-factors.

The average *B*-factor for the room temperature structure (2ALP) is 14.3 Å^2 for all atoms and 14.0 Å^2 for the main chain. A plot of the *B*-factor versus residue shows that there is considerable variation from the average, with the peaks occurring in large surface loops and minima appearing in the core (Fig. 3). The average *B*-factor decreased from 14.3 Å^2 at 298 K to 6 Å^2 at 120 K as measured by a Wilson plot (data not shown), or to 5.4 Å^2 as judged by the atomic *B*-factors. With the exception of four limited regions (5% of the atoms), described below, the *B*-factors at 120 K vary from the mean by only 3 Å^2 or less, suggesting that a majority of the *B*-factor variation at room temperature is due to differences in thermal fluctuations (Fig. 3A,B), and that, as observed in myoglobin (Hartmann et al., 1982), lattice disorder does not contribute significantly to the observed *B*-factors. The average *B*-factor at 298 K corresponds to an RMS displacement of 0.4 Å, whereas the 120 K *B*-factor corresponds to an RMS value of 0.2 Å, close to the zero-point value observed for small molecules (Willis & Pryor,

Table 3. *Low-temperature data for several proteins in increasing order of helical content*

	αLP	Trypsin[a]	Rnase-A[b]	HEWL[c]	Myoglobin[d]
Helical content (%)	4.5	9.4	27	46	67
Residues (#)	198	223	124	129	153
Low temperature (K)	120	120	98	100	80
Change in cell lengths (%)	0.8	1.0	0.6–2.7	1.0–2.8	1.04
Change in cell volume (%)	1.5	3.1	4.7	4.8	5
Change in radius of gyration (%)	0.13	0.25	0.7	0.93	1.04
Change in surface area (%)	−0.3	1.2	0.8[e]	1.8[f]	2.3
⟨T.E.C. (× 10^{-6} K^{-1})⟩[g]	13	n/a	n/a	40[h]	50
⟨T.E.C. (300 K)⟩[g]	24	n/a	n/a	n/a	115
Change in crystal contacts (# res.)[i]	9	[j]	10[k]	3[l]	~6[k]
B-factors (RT) (Å^2)	14.3	26.4	15.7	15.2	14
B-factors (LT) (Å^2)	5.4	9.6	6.6	8.1	5

[a]Earnest et al. (1991).
[b]Ribonuclease-A (Tilton et al., 1992).
[c]Hen egg white lysozyme (Young et al., 1994).
[d]Frauenfelder et al. (1987).
[e]Calculated from reported value of 0.4%/100 K for the protein volume.
[f]Percent change in volume.
[g]Thermal expansion coefficient, calculated according to Frauenfelder et al. (1987) (see text).
[h]Kurinov and Harrison (1995).
[i]Change in the number of residues < 4.0 Å from another molecule in the crystal (LT − RT).
[j]Slight increase from room temperature.
[k]4.5-Å cutoff distance.
[l]6.0-Å cutoff from geometric centroid of residue.

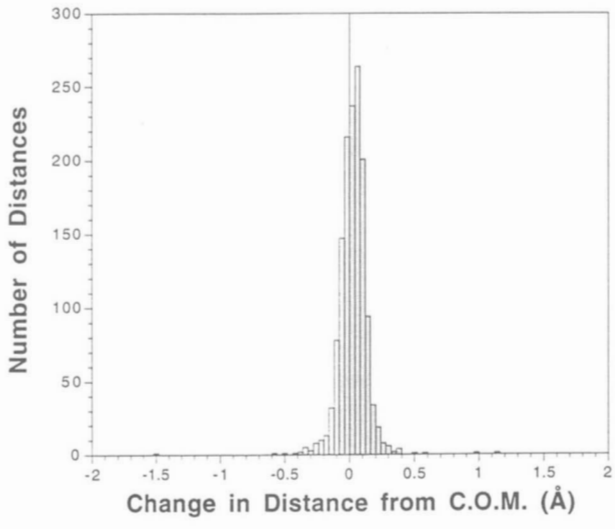

Fig. 2. Measures of thermal expansion in α-lytic protease using interatomic distances. Histogram of difference distances for each atom relative to the center of mass of the protein. For the structures at 298 and 120 K, all distances were measured from non-hydrogen protein atoms to the center of mass. The difference in this distance (298 K − 120 K) was calculated for each atom, and the resulting difference distances are shown. The location of the mean at a positive value indicates an expansion of the protein on heating.

1975). This supports the view that there is little lattice disorder in crystals of α-lytic protease, because rotational disorder would lead to higher *B*-factors at the surface and translational disorder would lead to higher *B*-factors throughout the protein. Two of the four regions with *B*-factors at least 1.5σ higher than the mean (as high as 19.4 Å^2; see Fig. 3) are in surface loops and the other two are strands that form part of the active site (residues 201A–207 and 216–225). These residues were considered potential locations for multiple conformations (see below).

Although the region of increased *B*-factors is suggestive of disorder, we wished to model optimally the underlying configurational heterogeneity. Although anisotropic *B*-factors provide information about the direction and amplitude of atomic motion, they can only model symmetric, harmonic ensembles of structures. An alternative strategy is to use multiple structures to model the configurational heterogeneity directly. As discussed, fixing the atomic *B*-factors to some uniform low value should force the models themselves to cover the configurational space. Because of the large increase in the number of free parameters for each model added, it is crucial to judge the ideal number of models to include (Fig. 4). Use of the free *R*-factor as a metric indicates that most of the improvement from adding additional coordinate sets is achieved with 4–6 structures, although the free *R*-factor continues to drop with as many as 16 structures. We have used the 16-structure refinement for analysis of conformational heterogeneity because it has the lowest free *R*-factor and gives the best sampling of coordinate space.

As a control, we also performed multiple conformation refinement in which the *B*-factors were allowed to vary. As measured by either the *R*-factor or the free *R*-factor, there is almost no difference in the quality of the resultant models. The structures generated without using a refined *B*-factor, however, sample conformational heterogeneity better as judged by the increase in RMSD of atomic coordinates from their mean value. With 16 different structures, the

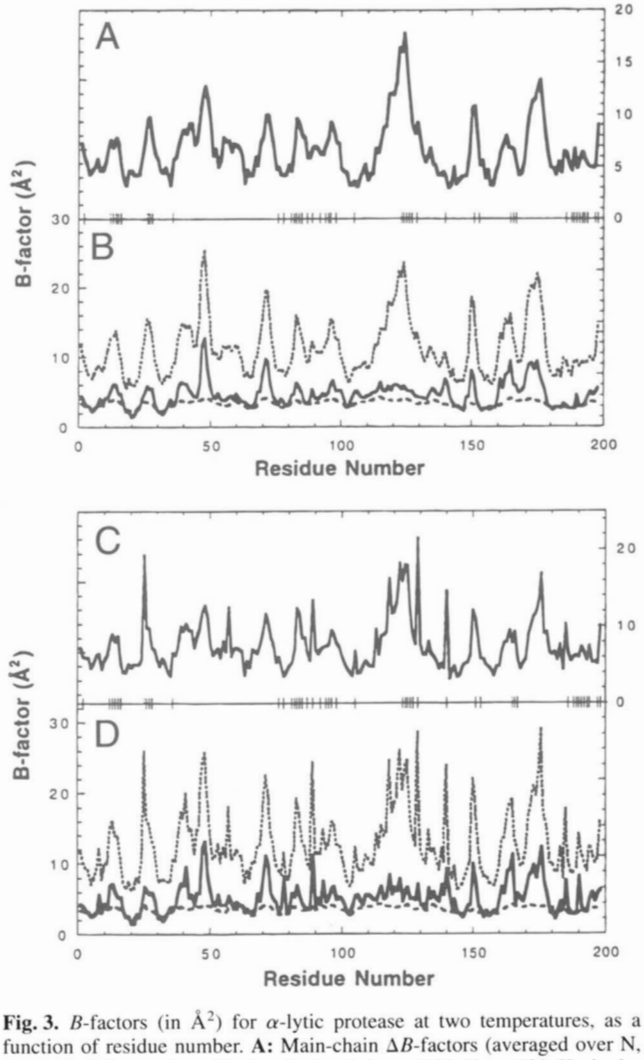

Fig. 3. *B*-factors (in Å^2) for α-lytic protease at two temperatures, as a function of residue number. **A:** Main-chain ΔB-factors (averaged over N, C_α, and C for each residue) calculated from (298 K − 120 K single-conformation). **B:** Main-chain *B*-factors for the 298 K structure (upper dashed line) and the 120 K model with a single structure (solid line) and with 16 conformations (lower dashed line). **C:** ΔB-factors (averaged over all atoms for each residue) calculated from (298 K − 120 K single-conformation). **D:** *B*-factors for the 298 K structure and 120 K structures (as above). Vertical bars on the center line indicate residues in crystal contacts.

difference between refining *B*-factors (RMSD = 0.30 Å) and not (RMSD = 0.32 Å) is small because the refined *B*-factors are fairly uniform (Fig. 3). This difference is accentuated if we consider only the regions that have high *B*-factors ($B > 8$ Å^2) at 120 K. In these regions, the average RMSD among the 16 structures is 0.43 Å when the *B*-factors are not refined, but only 0.40 Å when they are.

An example of the resulting $2F_o - F_c$ electron density from the multiple-conformation refinement is shown in Figure 5. The figure includes a region with large RMSDs (0.41 Å) and weak density, at Gly 216, and a region with low RMSDs (0.14 Å), at Tyr 171. However, 61 percent of the atoms have RMSDs less than 0.14 Å, indicating that the clustering of the multiple structures is very tight for the majority of the protein.

It is a remarkable indication of the robustness of this method that the *B*-factors in the multiple-conformation model fall to a low and rather uniform level, when refined in the control experiment

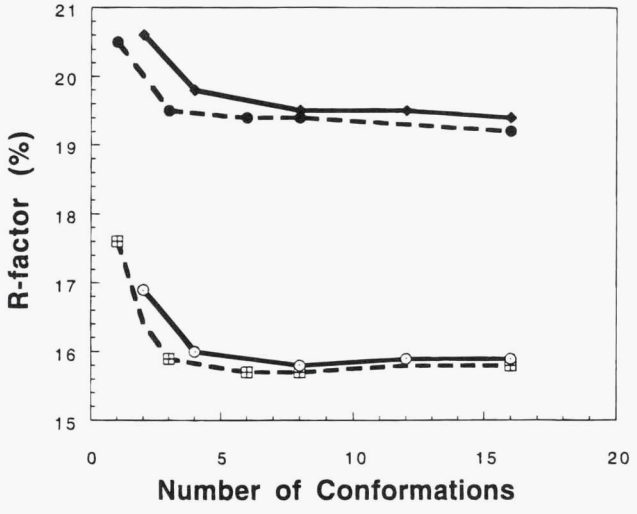

Fig. 4. Free *R*-factor (top) and conventional *R*-factor (bottom) as a function of the number of conformations in the multiple-conformation refinement. Solid lines represent *R*-factors for fixed atomic *B*-factors and dashed lines correspond to the refined *B*-factor control experiments. Refinement of atomic *B*-factors gives almost identical results to keeping all *B*-factors equal to the mean *B*-factor, supporting the view that *B*-factors need not be refined in a multiple conformation structure.

(Fig. 3A). The *B*-factors at the start of refinement were taken from the single-conformation structure and ranged from 1–13 Å^2 for the main chain. After refinement, the main-chain *B*-factors are all within the range of 2–4.5 Å^2. This result, in itself, indicates that conformational heterogeneity is being modeled by the spread of atomic coordinates and that *B*-factors are relatively insignificant to the model.

The multiple conformation data address another issue, namely how correct the *B*-factor is generally as a model of atomic displacements. If the models and the *B*-factors were modeling the identical probability distribution, the RMSD and the *B*-factors should be perfectly correlated. The lack of a perfect correlation, as shown in Figure 6, indicates that the multiple conformations are not simply sampling an ideal gaussian distribution. Although it is possible such deviations from ideality are a consequence of "noise fitting," the fact that both the *R*-factor and free *R*-factor decrease substantially upon inclusion of additional models indicates strongly that there is information in the X-ray data that is best represented by multiple conformations.

This point is reinforced by a consideration of the assumptions inherent in the *B*-factor model. Both isotropic and anisotropic *B*-factors contain in their parameterization the assumption of a harmonic electron density distribution, i.e., that it falls off monotonically and symmetrically from the maximum density. Figure 7 displays representative distributions of main-chain and side-chain angles from the 16-conformer refinement of the 120 K structure. Each plot has 16 points, corresponding to the 16 conformations of a particular residue (either in ϕ-ψ angles or in χ1-χ2 angles for side chains). The distributions of angles were classified according to their spread and symmetry as tight clusters, discrete clusters, symmetrically spread distributions, and asymmetrically spread dis-

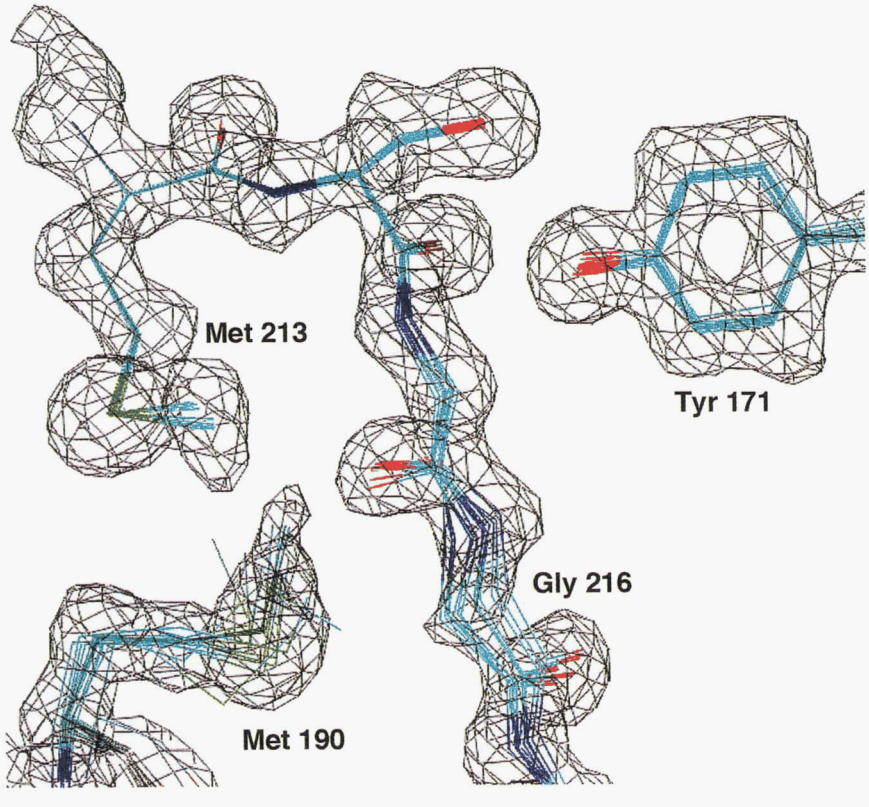

Fig. 5. Electron density in the active site of α-lytic protease. Density is contoured at 1.0 * sigma and shows the difference between a region with conformational substates (Gly 216, models spread out) and a region with a single conformation (Tyr 171, models clustered). Atoms are colored according to atom type: light blue, C; dark blue, N; red, O; green, S.

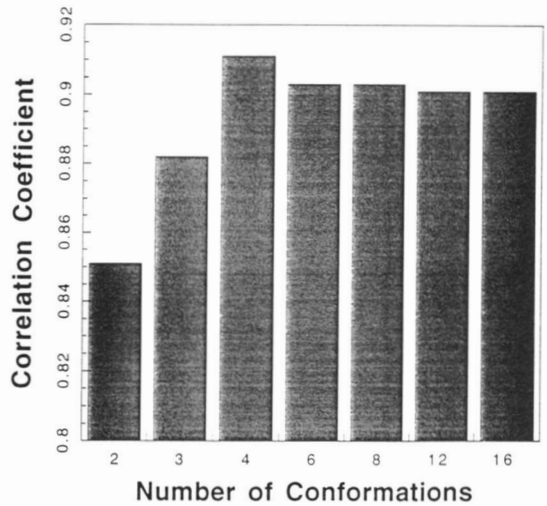

Fig. 6. Correlation between 120 K single-conformation *B*-factors and multiple-conformation RMSDs as a function of the number of structures. RMSDs were calculated directly from the *B*-factors in the single structure model. In the multiple structure models, the RMSDs from the mean position for each atom were calculated. The overall correlation coefficient between the RMSDs is shown. Lack of improvement of the correlation coefficient for more than four structures (coupled with the drop in free *R*-factor, Fig. 4) indicates that multiple conformation structures contain new information not present in the isotropic *B*-factor model.

tributions; an example of each of the four classes is shown in Figure 7. Table 4 shows that the positional heterogeneity of as many as 40% of the residues in α-lytic protease are not modeled well by isotropic *B*-factors in that the distribution of conformations is either asymmetric or anharmonic (seen most clearly in the discrete clusters). Such clusters would not be well-modeled by anisotropic *B*-factors either (which were not used here), which still assume a harmonic distribution. Therefore, multiple conformation refinement provides the best model of conformational heterogeneity.

It has been proposed that flexibility is important for function. Correlated motions are probably the more relevant dynamic property. Figure 8 shows the subset of structures from the 16-structure refinement in which the correlated motion of residues across the P1 binding pocket is most obvious. The geometry of the binding pocket is apparently organized so that a shift to the left at Gly 216 is accompanied by a similar shift at Met 190 and at Arg 192. Even though all of these residues can move, they appear to do so in a coordinated fashion that maintains their close interactions. We have termed this phenomenon "dynamic close packing."

Discussion

Structure at 120 K

Analysis of the structure of αLP at 120 K indicates remarkably little thermal expansion. Although this unusual rigidity is in line with predictions for β-sheet proteins (Tilton et al., 1992; Young et al., 1994), due to reduced segmental accommodation of β-sheet structures compared to α-helices, it is also possible that it is a consequence of the unique stability of αLP. However, in examining the limited set of published structures determined at room and cryogenic temperatures, a variety of properties seem to vary monotonically with fraction helix (Table 3). This suggests that reduced thermal expansion may be a general property of β-sheet proteins.

Crystal contacts are often invoked as a perturbing force to explain differences between crystal structures and solution structures, and on separate occasions have been observed to either increase or decrease the order of the affected regions (Kossiakoff et al., 1992; Young et al., 1994). The data in Figure 3 suggest that, in the case of αLP, the effect of crystal contacts on *B*-factors is insignificant. Although the average 120 K *B*-factor for atoms in crystal contacts (6.7 Å^2) is slightly higher than the average for all atoms (5.4 Å^2), three of the four regions with the highest *B*-factors are not at crystal contacts. Furthermore, a number of atoms at crystal contacts have extremely low *B*-factors. The data also argue against a reduction in *B*-factors by the crystal contacts: 86 of 144 atoms (60%) involved in crystal contacts in the single-structure 120 K model have *B*-factors higher than the mean for all atoms, indicating that they are not rigidified by crystal contacts. Moreover, the average ΔB (see below) for all atoms involved in intermolecular contacts (9.5 Å^2) indicates that they have a significant amount of mobility and are not particularly rigidified (Fig. 3). These results contrast with observations made by Young et al. (1994) on hen egg-white lysozyme, where they found that atoms in crystal contacts have *B*-factors and ΔB-factors lower than the average. This difference may be a consequence of the extreme rigidity of αLP.

Conformational substates and plasticity

The low-temperature study of α-lytic protease was undertaken in order to determine whether flexibility or plasticity plays an important role in enzyme specificity. Initial studies of α-lytic protease complexed to a transition-state analogue suggested that the protein provided a rigid template for the hydrolytic transition state (Bone et al., 1987). Subsequent investigations of complexes with inhibitors corresponding to nonoptimal substrates revealed that, although the catalytic machinery stays rigid, the protein actually has a large number of available conformations with which to accommodate substrates (Bone et al., 1989a, 1989b, 1991a; Mace & Agard 1995; Mace et al., 1995b), in agreement with the induced fit model of substrate binding. The additional conformational states are not evident in the native enzyme or in the uncomplexed mutants, either as explicit alternative conformations in the electron density, or as high *B*-factors, but the kinetic data indicate that they must be accessible without large energetic cost. The presence of multiple conformational substates in a rigid molecule has been described as plasticity to differentiate it from flexibility (Fig. 1). All of these data suggested a direct link between protein dynamics and function, which we hoped to substantiate with the low-temperature study.

Plasticity is defined relative to a characteristic relaxation temperature (T_r) of the atoms in question. At temperatures $T << T_r$, the barriers between conformational substates will be too high to be crossed and atoms will be trapped in a single substate (Fig. 1). Under these conditions, a protein should have low *B*-factors as long as multiple conformations are modeled explicitly, or if a single model is modeling just one of the substates. At temperatures $T >> T_r$, the substates will be sampled freely and atoms effectively will see a single potential well, possibly leading to high *B*-factors and apparent flexibility, depending on the resolution of the experiment and the separation of the substates. It is only in an intermediate range of temperatures, with T near T_r, that plasticity should be apparent, i.e., that the *B*-factors should reflect a narrower potential well than is in fact accessible.

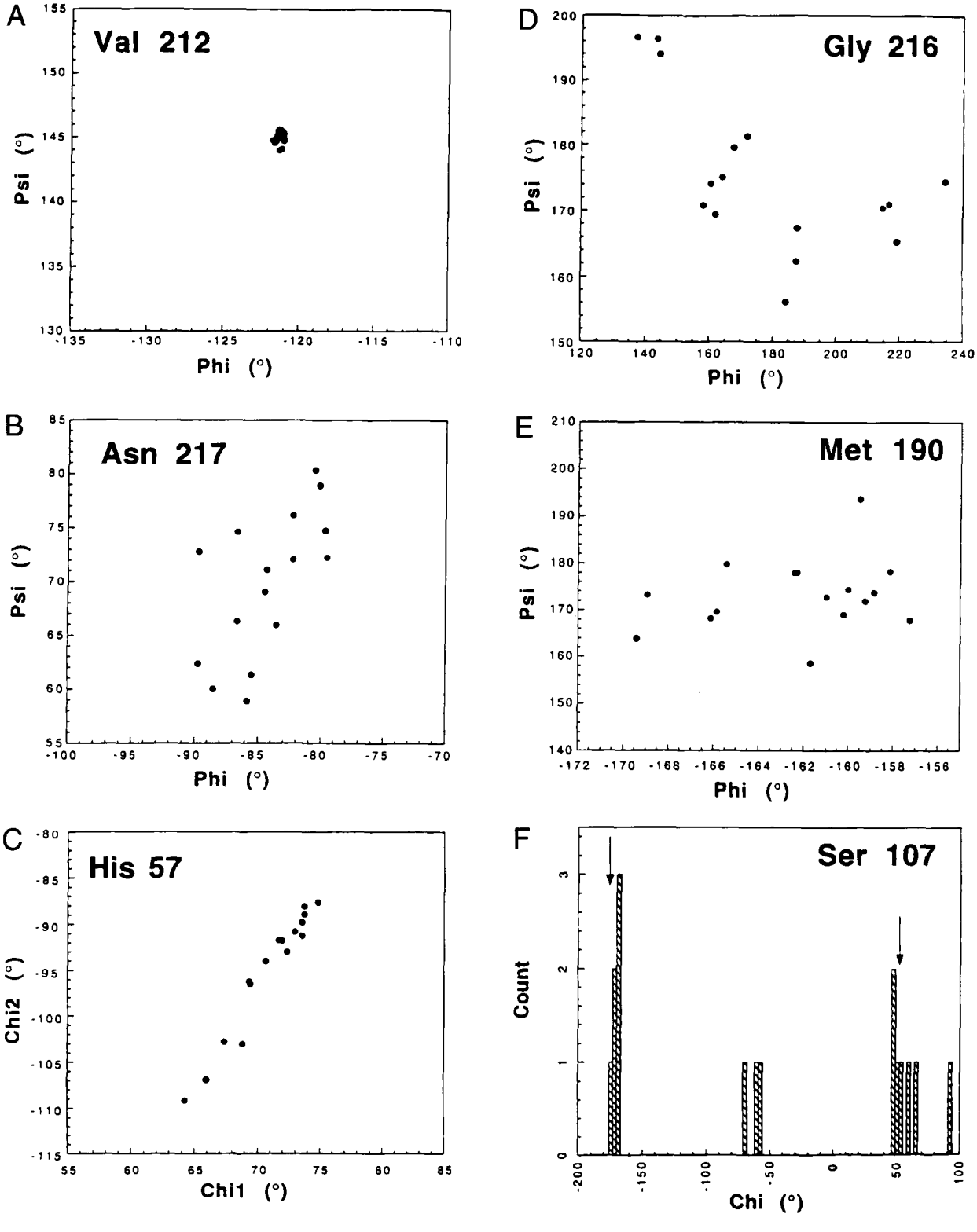

Fig. 7. Ramachandran and $\chi 1$-$\chi 2$ plots from multiple conformation refinement at 120 K. Each point represents one of the 16 conformations in the multiconformation refinement. **A,B,C:** Examples of clustered, symmetrically spread, and asymmetrically spread distributions, respectively. The residue is indicated for each plot. **D,E:** Two examples of distributions with discrete clusters. **F:** Histogram of chi angles from the single-conformation and multiple-conformation refinements. This residue had discrete side-chain conformations in the single-conformation model (arrows). The multiple-conformation structures cluster around these positions, but include others as well.

Table 4. *Occurrence of distribution classes for backbone and side-chain angles in multiple conformation (16 structures) refinement*

	Backbone	Side-chain
Tight clusters	35 (18)	46 (33)
Symmetric spread	82 (42)	37 (26)
Asymmetric spread	62 (32)	44 (31)
Discrete clusters	16 (8)	14 (10)

[a]Values in parentheses are percentages of measured conformations.

Remarkably, we find that many of the regions that are perturbed so easily by inhibitor binding also exhibit multiple conformational substates at low temperature, each of which is in a local energy minimum. There is a large enough barrier between the substates at 120 K that intermediate conformations are minimally populated (Figs. 1, 7). Smith et al. (1986) also found evidence for conformational substates in their investigation of four high-resolution structures and concluded that discrete conformations are preferred over continuous variations. Furthermore, studies of myoglobin (Leeson & Wiersma, 1995) and cytochrome *c* (Leeson et al., 1994) reveal hierarchical levels of conformational substates that are distinguishable at low temperatures. The results presented here demonstrate a correlation between the conformational energy surface of residues in the active site of the free enzyme and the positional variation of those residues among the structures of the enzyme complexed with bound inhibitors.

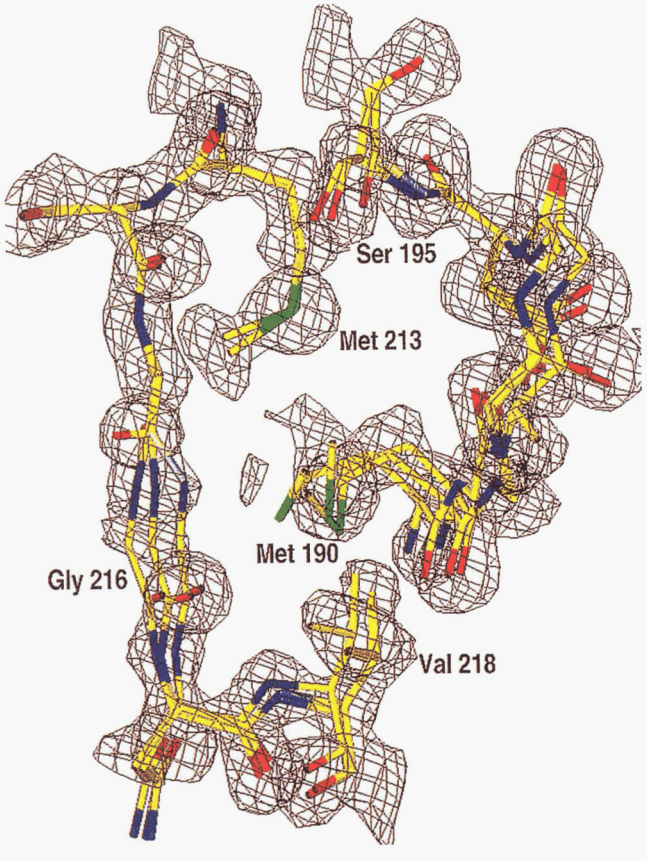

Fig. 8. Correlated motions in the binding pocket of α-lytic protease. This subset of structures from the 16-conformation refinement shows correlation in atomic positions across the residues of the P1 binding pocket. The atoms from the same structure (e.g., Gly 216 C_α from structure 14 and Met 190 C_α from structure 14, leftmost structure) are shifted in the same direction relative to the mean position for each atom, suggesting that residues across the binding pocket are not moving independently. Atoms are colored according to atom type: yellow, C; dark blue, N; red, O; green, S.

Multiple-conformation modeling and refinement of B-factors

Our goal is to extract as much detailed information on the conformational substates from the low-temperature X-ray diffraction data as possible. Unfortunately, isotropic *B*-factors provide only a crude estimate of molecular motion. Experiments indicate that positional heterogeneity is anharmonic and asymmetric (Cusack & Doster, 1990), particularly in the case of multiple side-chain conformations (Smith et al., 1986; Earnest et al., 1991; Tilton et al., 1992), and hence cannot be well described by isotropic *B*-factors. Furthermore, in a recent normal mode analysis of bovine pancreatic trypsin inhibitor, Hayward et al. (1995) found that 98% of the total mean square fluctuations are accounted for by anharmonic motions. Although anisotropic *B*-factors could be used, a better representation of conformational heterogeneity is an explicit model in which multiple structures are refined simultaneously. We argue that the multiple-conformation model presented here in which the *B*-factors are not refined results in a more accurate model than a multiple-conformation model with refined *B*-factors. Fixing the *B*-factors in a multiple conformation refinement is required to ensure that the intrinsic conformational heterogeneity is modeled explicitly. The importance of explicit modeling is shown in Figure 7 and Table 4. A significant number of residues in α-lytic protease have discrete distributions, which cannot be approximated by *B*-factors, even anisotropic ones, and may underlie the plasticity observed in previous structures of α-lytic protease.

Multiple-conformation refinement, although a powerful method, is expensive in terms of extra parameters in the model. Although the apparent ratio of parameters to observations is greater than unity [there are 66,768 parameters for the Cartesian coordinates of the protein atoms in the 16 models (Table 2) and 31,458 unique reflections (Table 1)], the actual number of observations is augmented significantly by the stereochemical restraints applied to each of the models. It is generally recognized that geometric restraints provide a great reduction in the number of free parameters. The observations below confirm the validity of this assumption.

As in previous work (Burling et al., 1996), we have used the free *R*-factor to determine the optimal number of conformations to use in the refinement. Surprisingly, this shows that the model does not over-fit the data, even with 16 structures (Fig. 4). Not only is the multiple-conformation model acceptable, as indicated by the free *R*-factor, but it is also robust, as shown by the drop in *B*-factors to a nearly uniform level when they were refined in our control experiment (Fig. 3A). Even when the *B*-factors are allowed to vary, effectively all of the conformational heterogeneity is modeled directly by the spread of the structures rather than implicitly in the *B*-factors.

The question remains as to whether there are a few structures, outliers, that contribute to the high RMSDs and are simply fitting noise. The RMSD of 73.1% of the atoms is 0.30 Å or less, suggesting that the models are not fitting noise. Many of the regions with high RMSDs do not consist of a cluster of positions with a

few outliers, but instead are spread over the whole range (Fig. 7). As a more stringent test of the possible role of outliers, we removed the two atoms farthest from the mean for each position in the protein and recalculated the RMSDs. The correlation coefficient between this RMSD and the original one is 0.970 (data not shown), indicating that the RMSDs accurately reflect the spread of all the models and are not biased by outliers. In addition, the RMSDs correlate well with the *B*-factors (Fig. 6), indicating that both are modeling real structural features. Importantly, the discrete side-chain conformations seen at 120 K where the data to parameter ratio is excellent are reproduced accurately in the multiple conformation model (Fig. 7F).

Correlated motion in proteins

The dynamic nature of proteins is not usually evident in X-ray crystallographic analysis, but proteins are known to be highly flexible at physiological temperatures. Indeed, many proteins require a certain amount of flexibility to carry out their biological function (Frauenfelder et al., 1991; Rasmussen et al., 1992; Leeson & Wiersma, 1995). Flexibility is used, for example, by enzymes to clamp around their substrates, thereby excluding solvent and isolating potentially reactive intermediates. Although random atomic motions are critical for protein function, correlated motions in which neighboring atoms (bonded and nonbonded) move in unison should be considerably more effective. It is not surprising that correlated motions should occur in the tightly packed interior of proteins, where steric effects might force small domains of atoms to move together. This effect would result in the ability of a protein to maintain the degree of rigidity necessary to bind small substrates, for example, while still having enough flexibility to accommodate larger ones.

Unfortunately, it has not been possible to observe correlated motions in proteins directly [except, to a limited extent, by thermal diffuse scattering of X-rays (Doucet & Benoit, 1987; Caspar et al., 1988; Thune & Badger, 1995)]. Although experimental results are often suggestive of correlated motions, the best evidence for their existence comes from calculations, either normal mode analysis, in which the vibrational modes are calculated directly, or via molecular dynamics. Thus, our observation of correlated motions in the multiple-conformation model was unexpected. However, the energetic benefit for atoms in the binding pocket to maintain their tight packing as they move ("dynamic close packing") may provide a suitable explanation for this phenomenon.

Mace and Agard (1995) previously have reported data that suggested the possibility of correlated motions in the active site of α-lytic protease. The observations presented here provide the first evidence for their existence. The close packing of the binding pocket implied by this observation explains the specificity of the wild-type protease toward substrates with small side chains at the P1 position. Because the atomic motions are correlated, they exhibit plasticity without reducing the specificity of the enzyme. It is also clear how mutating Met 190 to alanine could disrupt the correlation between motions on the two sides of the pocket, leading to surprisingly large changes in the specificity profile of the enzyme (Bone et al., 1989b). Along with providing more volume for a substrate side chain to fit in, this change might decrease the specificity of the enzyme by allowing different parts of the binding pocket to move independently of each other to accommodate a wide variety of substrate side chains.

Although the role of local dynamics in protein function has been reviewed frequently (Ringe & Petsko, 1986; Frauenfelder et al., 1991; Thune & Badger, 1995), there is very little experimental evidence for it outside of ligand binding in myoglobin, hemoglobin, and cytochrome *c*. The plethora of structure–function studies on α-lytic protease provide an opportunity to relate its dynamic behavior to well-characterized aspects of its function, such as its substrate specificity. We have presented evidence here for the presence of conformational substates that may explain the plasticity seen in α-lytic protease. We have also presented evidence for correlated motions in the P1 binding pocket of α-lytic protease. Currently, we are comparing the results of NMR relaxation experiments with the crystallographic data to see whether these very different techniques reveal a similar view of the dynamics of the active site.

Materials and methods

Purification and crystallization

Wild-type α-lytic protease was purified as described in Bone et al. (1987). The protein was crystallized by serial dilution seeding of drops containing 20 mg/mL protein (5 μL protein plus 5 μL precipitant) that had been equilibrated over wells containing 1.3 M Li_2SO_4 and 20 mM Tris-SO_4, pH 7.5, for 48 h (Bone et al., 1987). Crystals grew from the seeds in 3–4 weeks. The crystals lie in space group $P3_221$ with unit cell dimensions $a = b = 66.3$, $c = 80.1$ (Brayer et al., 1979).

Low-temperature data collection

A 0.3 × 0.15 × 0.08 mm crystal was transferred to a cryosolvent consisting of the precipitant solution plus 15% glycerol. After 2 min of equilibration, the crystal was suspended in a 75-μ-thick nichrome wire loop (0.7-mm diameter) by touching the loop to the inverted drop containing the crystal and then wicking away excess cryosolvent. The crystal was frozen by rapid insertion into a stream of dry nitrogen gas cooled to 120 K by passage through a dewar of liquid nitrogen. Data were collected on a MAR Research image plate detector at the Stanford Synchrotron Radiation Laboratory using X-rays with $\lambda = 1.08$ Å. Data were collected in 2.5° oscillation frames and reduced with the Denzo package (CCP4, 1979) on a Vax 9000 computer. Scaling and averaging were performed with the Rotavata and Agrovata programs (CCP4, 1979). Spots were visible to the edge of the detector (1.38 Å), but the data did not satisfy our quality criteria ($I/\sigma > 2.5$ for 50% of the reflections) beyond 1.5 Å. The R_{sym} for all data to 1.5 Å is 5.9% (24% in the highest resolution shell, 1.57–1.50 Å, see Table 1), and the data are 98.95% complete (99.11% in the highest resolution shell).

Structure refinement—Single conformation

We started the refinement of the 120 K wild-type structure with the refined 1.7 Å structure of α-lytic protease (2ALP, Fujinaga et al., 1985). The initial *R*-factor was 35%. The model was refined with X-PLOR (Brünger, 1992) to a final *R*-factor of 16.5% (free *R*-factor = 19.2%) (Table 2). Several cycles of hand-building and addition of waters were performed with FRODO (Jones, 1982) in maps with coefficients ($2F_o - F_c$) and ($F_o - F_c$) and phases from the model. Water molecules were inserted into difference electron density peaks greater than 5 * σ and were kept if their occupancy

was above 0.1 and their *B*-factor less than 45 Å^2. Individual *B*-factors for all atoms and occupancies for solvent atoms were refined in alternate cycles with X-PLOR. In the current work, only isotropic *B*s were refined. Alternate side-chain conformations were modeled when visible in electron density maps (both $F_o - F_c$ and $2F_o - F_c$) and confirmed by omit maps and model parameters. Only alternate conformations with occupancies of at least 0.2 and *B*-factors lower than 25 Å^2 were modeled.

Structure refinement—Multiple conformations

Multiple-conformation refinement was performed as described by Burling et al. (1996) and Kuriyan et al. (1991). The refined 120 K single conformation was used as the starting model for multiple conformation refinement, but the *B*-factors of the protein atoms were all set to the mean *B*-factor for the backbone protein atoms (3.47 Å^2) to ensure that the structures were sampling any conformational heterogeneity optimally (see Discussion). Two to 16 identical copies of this structure were made within X-PLOR (Brünger, 1992) and the occupancies of all the atoms were set to the reciprocal of the number of structures. Restraints were imposed such that each structure interacted only with itself and with solvent atoms, and the structures were then allowed to diverge during the course of a slow cooling and minimization protocol. This involved (1) determining the weight for the X-ray terms in the molecular dynamics, (2) 40 cycles of minimization, (3) simulated annealing from 500 K to 0 K in 20 K steps with 50 dynamics steps at each temperature, (4) 40 cycles of minimization, (5) optimization of the overall *B*-factor and individual *B*-factors for the solvent, and (6) 40 cycles of minimization. After the optimal number of conformations had been determined from the free *R*-factor (using 10% of the data), a control was done in which the individual *B*-factors from the single refined structure were retained in the multiple models and optimized after slow cooling. Although multiple conformations were used for the protein, only a single conformation, for which we refined *B*-factors and occupancies, was used for the solvent. The solvent model was completed by several rounds of building into $F_o - F_c$ electron density and examination of the resulting maps and atomic parameters.

Data analysis

The surface area of the protein was determined with the program ACCESS (Richards, 1977). To determine the thermal component of the temperature factors, differences were taken between the *B*-factors at 298 K and those at 120 K, using 2ALP as the 298 K model. RMSDs between structures were calculated with Lsqman (Kleywegt, 1994). Some statistics on *B*-factors were calculated with Moleman (Kleywegt, 1995). Graphs were created with Kaleidagraph (Abelbeck Software, Reading, PA) on a PowerMac 7100/80.

The heterogeneity of structures was quantified in several ways. RMSDs were calculated relative to the mean structure using X-PLOR (Brünger, 1992). A Ramachandran plot was made for each residue, using data from all 16 structures, and these distributions of main-chain phi and psi angles were classified according to their spread and asymmetry. Four classes were used: tight clusters (all points within 2° of each other), symmetrically spread distributions, discrete clusters (two or more clusters separated by 5° or more), and asymmetric distributions. Side-chain angles $\chi 1$ and $\chi 2$ were plotted and classified in the same way using a function of the IVE platform (Chen et al., 1996).

Acknowledgments

This work was supported by funds from the Howard Hughes Medical Institute (D.A.A.). S.D.R. was supported by NIH training grant GM08284. The Stanford Synchrotron Radiation Laboratory is funded by the Department of Energy, Office of Basic Energy Science. The biotechnology program is supported by the National Institutes of Health, Biomedical Research Technology Program, National Center for Research Resources. Further support is provided by the Department of Energy, Office of Health and Environmental Research. We thank Roger Bone for early discussions of this work, and Tom Earnest and Chuck Wilson for help with the low-temperature crystallography. The coordinates for the single- and multiple-conformation structures presented here have been deposited with the Brookhaven Protein Data Bank and have accession codes 1TAL and 2ULL, respectively.

References

Alber T, Gilbert WA, Ponzi DR, Petsko GA. 1983. The role of mobility in the substrate binding and catalytic machinery of enzymes. *Ciba Found Symp 93*:4–24.

Bone R, Frank D, Kettner CA, Agard DA. 1989a. Structural analysis of specificity: Alpha-lytic protease complexes with analogs of reaction intermediates. *Biochemistry 28*(19):7600–7609.

Bone R, Fujishige A, Kettner CA, Agard DA. 1991a. Structural basis for broad specificity in alpha-lytic protease mutants. *Biochemistry 30*(43):10388–10398.

Bone R, Sampson NS, Bartlett PA, Agard DA. 1991b. Crystal structures of alpha-lytic protease complexes with irreversibly bound phosphonate esters. *Biochemistry 30*(8):2263–2272.

Bone R, Shenvi AB, Kettner CA, Agard DA. 1987. Serine protease mechanism: Structure of an inhibitory complex of alpha-lytic protease and a tightly bound peptide boronic acid. *Biochemistry 26*(24):7609–7614.

Bone R, Silen JL, Agard DA. 1989b. Structural plasticity broadens the specificity of an engineered protease. *Nature 339*(6221):191–195.

Brayer GD, Delbaere LT, James MN. 1979. Molecular structure of the alpha-lytic protease from Myxobacter 495 at 2.8 Ångstroms resolution. *J Mol Biol 131*(4):743–775.

Brünger AT. 1992. *X-PLOR: A system for X-ray crystallography and NMR*. New Haven, Connecticut: Yale University Press.

Burling FT, Weis WI, Flaherty KM, Brünger AT. 1996. Direct observation of protein solvation and discrete disorder with experimental crystallographic phases. *Science 271*(5245):72–77.

Caspar DL, Clarage J, Salunke DM, Clarage M. 1988. Liquid-like movements in crystalline insulin. *Nature 332*(6165):659–662.

CCP4. 1979. *Collaborative Computing Project No. 4. A suite of programs for protein crystallography*. Warrington, UK: SERC Daresbury Laboratory.

Chen H, Hughes DD, Chan TA, Sedat JW, Agard DA. 1996. IVE (Image Visualization Environment)—A software platform for all three-dimensional microscopy applications. *J Struct Biol 116*(1):56–60.

Cusack S, Doster W. 1990. Temperature dependence of the low frequency dynamics of myoglobin. Measurement of the vibrational frequency distribution by inelastic neutron scattering. *Biophys J 58*(1):243–251.

Doucet J, Benoit JP. 1987. Molecular dynamics studied by analysis of the X-ray diffuse scattering from lysozyme crystals. *Nature 325*(6105):643–646.

Earnest T, Fauman E, Craik CS, Stroud R. 1991. 1.59 Å structure of trypsin at 120 K: Comparison of low temperature and room temperature structures. *Proteins Struct Funct Genet 10*(3):171–187.

Frauenfelder H, Hartmann H, Karplus M, Kuntz ID Jr, Kuriyan J, Parak F, Petsko GA, Ringe D, Tilton RF Jr, Connolly ML et al. 1987. Thermal expansion of a protein. *Biochemistry 26*(1):254–261.

Frauenfelder H, Petsko GA, Tsernoglou D. 1979. Temperature-dependent X-ray diffraction as a probe of protein structural dynamics. *Nature 280*(5723):558–563.

Frauenfelder H, Sligar SG, Wolynes PG. 1991. The energy landscapes and motions of proteins. *Science 254*(5038):1598–1603.

Fujinaga M, Delbaere LT, Brayer GD, James MN. 1985. Refined structure of alpha-lytic protease at 1.7 Å resolution. Analysis of hydrogen bonding and solvent structure. *J Mol Biol 184*(3):479–502.

Hartmann H, Parak F, Steigemann W, Petsko GA, Ponzi DR, Frauenfelder H. 1982. Conformational substates in a protein: Structure and dynamics of metmyoglobin at 80 K. *Proc Natl Acad Sci USA 79*(16):4967–4971.

Hayward S, Kitao A, Go N. 1995. Harmonicity and anharmonicity in protein dynamics: A normal mode analysis and principal component analysis. *Proteins Struct Funct Genet 23*(2):177–186.

Jones TA. 1982. FRODO. In: Sayre D., ed. *Computational crystallography*. Oxford, UK: Oxford University. pp 303–317.

Kettner CA, Bone R, Agard DA, Bachovchin WW. 1988. Kinetic properties of the binding of alpha-lytic protease to peptide boronic acids. *Biochemistry 27*(20):7682–7688.

Kleywegt GJ. 1994. A super position. In: *ESF/CCP4 Newsletter*. pp 9–14.

Kleywegt GJ. 1995. Dictionaries for heteros. In: *ESF/CCP4 Newsletter*. pp 45–50.

Kossiakoff AA, Randal M, Guenot J, Eigenbrot C. 1992. Variability of conformations at crystal contacts in bpti represent true low-energy structures: Correspondence among lattice packing and molecular dynamics structures. *Proteins Struct Funct Genet 14*:65–74.

Kurinov IV, Harrison RW. 1995. The influence of temperature on lysozyme crystals. Structure and dynamics of protein and water. *Acta Crystallogr D 51*:98–109.

Kuriyan J, Osapay K, Burley SK, Brünger AT, Hendrickson WA, Karplus M. 1991. Exploration of disorder in protein structures by X-ray restrained molecular dynamics. *Proteins Struct Funct Genet 10*(4):340–358.

Leeson DT, Berg O, Wiersma DA. 1994. Low-temperature protein dynamics studied by the long-lived stimulated photon echo. *J Phys Chem 98*:3913–3916.

Leeson DT, Wiersma DA. 1995. Looking into the energy landscape of myoglobin. *Nature Struct Biol 2*(10):848–851.

Mace JE, Agard DA. 1995. Kinetic and structural characterization of mutations of glycine 216 in alpha-lytic protease: A new target for engineering substrate specificity. *J Mol Biol 254*(4):720–736.

Mace JE, Wilk BJ, Agard DA. 1995. Functional linkage between the active site of alpha-lytic protease and distant regions of structure: Scanning alanine mutagenesis of a surface loop affects activity and substrate specificity. *J Mol Biol 251*(1):116–134.

Rasmussen BF, Stock AM, Ringe D, Petsko GA. 1992. Crystalline ribonuclease A loses function below the dynamical transition at 220 K [see comments]. *Nature 357*(6377):423–424.

Richards FM. 1977. Areas, volumes, packing and protein structure. *Annu Rev Biophys Bioeng 6*:151–176.

Ringe D, Petsko GA. 1986. Study of protein dynamics by X-ray diffraction. *Methods Enzymol 131*:389–433.

Schechter I, Berger A. 1967. On the size of the active site in proteases. I. Papain. *Biochem Biophys Res Commun 27*(2):157–162.

Smith JL, Hendrickson WA, Honzatko RB, Sheriff S. 1986. Structural heterogeneity in protein crystals. *Biochemistry 25*(18):5018–5027.

Thune T, Badger J. 1995. Thermal diffuse X-ray scattering and its contribution to understanding protein dynamics. *Prog Biophys Mol Biol 63*(3):251–276.

Tilton RF Jr, Dewan JC, Petsko GA. 1992. Effects of temperature on protein structure and dynamics: X-ray crystallographic studies of the protein ribonuclease-A at nine different temperatures from 98 to 320 K. *Biochemistry 31*(9):2469–2481.

Whitaker DR, Jurasek L, Roy C. 1966. The nature of the bacteriolytic proteases of *Sorangium* sp. *Biochem Biophys Res Commun 24*(2):173–178.

Willis BTM, Pryor AW. 1975. *Thermal vibrations in crystallography*. Cambridge, UK: Cambridge University Press.

Young AC, Tilton RF, Dewan JC. 1994. Thermal expansion of hen egg-white lysozyme. Comparison of the 1.9 Å resolution structures of the tetragonal form of the enzyme at 100 K and 298 K. *J Mol Biol 235*(1):302–317.